



# In situ biomanufacturing of artificial blood vessels via 3D bioprinting

Haitao Cui <sup>1</sup>, Margaret Nowicki <sup>1</sup>, and Lijie Grace Zhang <sup>1, 2, 3</sup>

<sup>1</sup>Department of Mechanical and Aerospace Engineering, <sup>2</sup>Department of Biomedical Engineering, <sup>3</sup>Department of Medicine, The George Washington University

## Introduction

The ability to fabricate artificial tissues/organs that recapitulate the multi-scale structural, mechanical, physicochemical and essential aspects of biological functions is highly critical for future clinical tissue and organ implantation applications. One significant challenge facing the development of large-scale artificial tissue for defect reconstruction is vascularization of the complex tissue implants. However, current researches fail to generate multi-scale, multilayer and independent blood vessels that replicate the geometry, complexity, and longevity of human vascularized tissues.

To satisfy the concomitant requirements, we developed an extrusion printer with a coaxial nozzle and a new printable cell-laden bioink to directly fabricate the blood vessel. The artificial blood vessel may be independently printed in any engineered tissue implant, which can transport oxygen and nutrients for the integrated matrix through perfused microcirculation.

## Materials and Characteristics

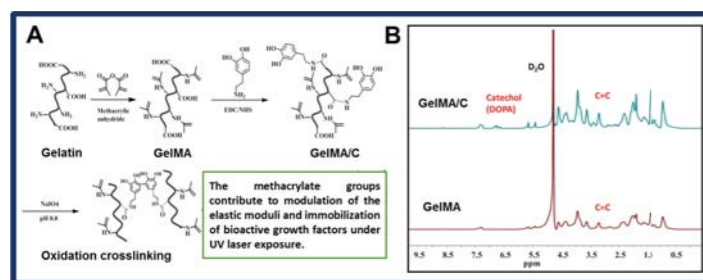


**Figure 1.** Preparation of bioink material. (A) synthesis route and (B) <sup>1</sup>H NMR spectra of gelatin methacrylate/catechol (GelMA/C). The bioink was synthesized through a two-step chemical reaction, in which gelatin was successively reacted with methacrylate and dopamine.

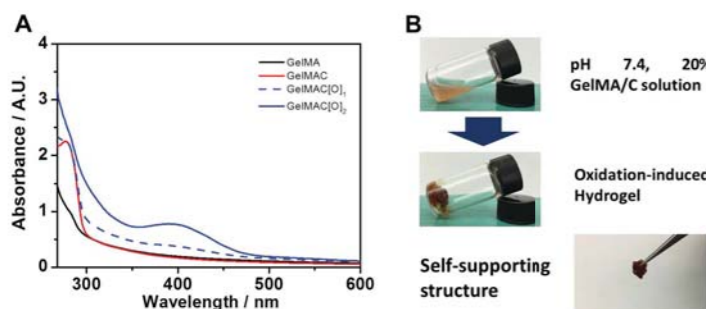


**Figure 2.** Crosslinking mechanism and hydrogel formation. (A) Oxidation-induced crosslinking study via UV-Vis spectra and (B) Self-supporting hydrogel formation.

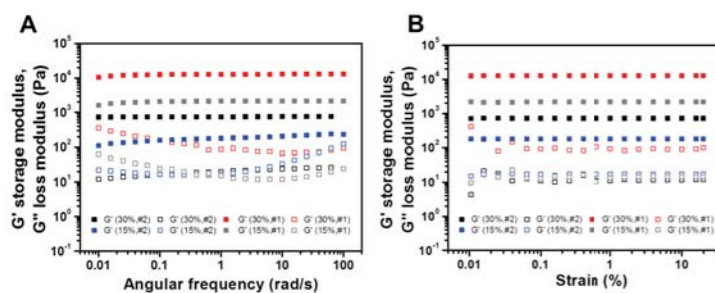


**Figure 3.** Rheological properties of the hydrogel, including angular frequency(A) and strain (B) tested using rheometer. Storage modulus and loss modulus changes with varying concentration and graft ratio of dopamine (#1: 3.2 w/w % and #2: 1.4 w/w%)

## Structural Design and Bioprinting

### Schematic of a Coaxial Extrusion Printer System

The bioprinting step was performed using a coaxial needle extrusion system, in which the bioink mixture containing GelMA/C, and smooth muscle cells (SMCs) flowed, through an external needle (20G, diameter: 910 μm) while the crosslinking solution F127/NaIO<sub>3</sub>, and human umbilical vein endothelial cells (HUVECs) flowed through the internal needle (26G, diameter: 500 μm). When the crosslinking solution came in contact with the bioink, the catechol groups of GelMA/C were rapidly cross-linked to form a self-supporting blood vessel with a bilayered cell structure.

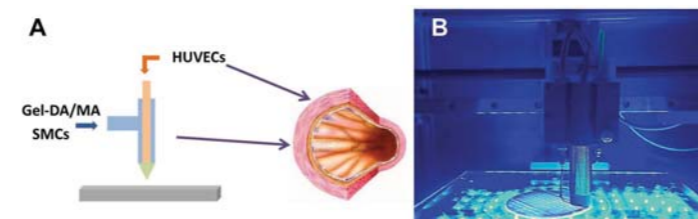


**Figure 4.** (A) Design of artificial blood vessel manufacturing, including smooth muscle cell layer (SMCs) and human umbilical vein endothelial cell layer (HUVECs). (B) Photo image of a coaxial extrusion bioprinting with dual bioinks.

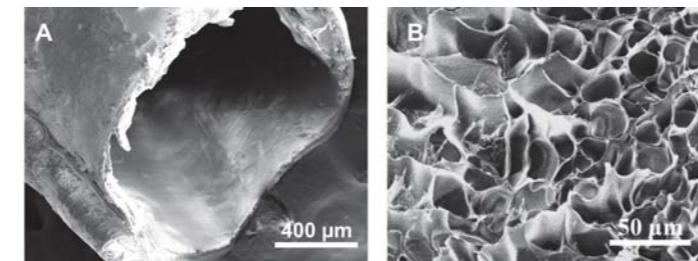


**Figure 5.** (A) Scanning electron microscope (SEM) image of a 3D bioprinted blood vessel. (B) Locally amplified SEM image of the blood vessel hydrogel.

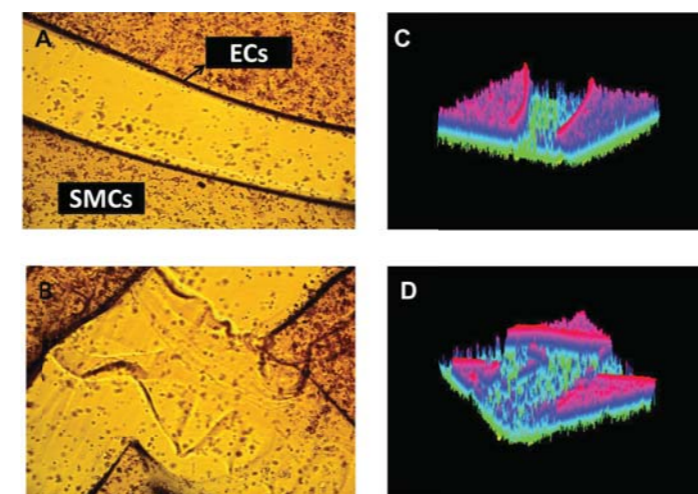


**Figure 6.** Light microscope images of 3D bioprinted blood vessels with (A) straight and (B) branched structures. Finite-element model predictions of the 3D bioprinted blood vessels with (C) straight and (D) branched structures.

## Cell-laden Bioprinting

### 3D Bioprinted Blood Vessel with SMCs/HUVECs

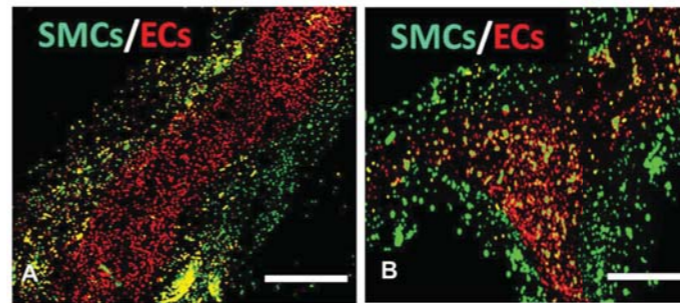


**Figure 7.** Confocal microscopy images of co-cultured SMCs and HUVECs in (A) straight and (B) branched blood vessel constructs for 7 days. SMCs were labeled with cell tracker green, and HUVECs were stained with cell tracker red. The scale bars indicate 500 μm.

## Cell Live/Dead Assay

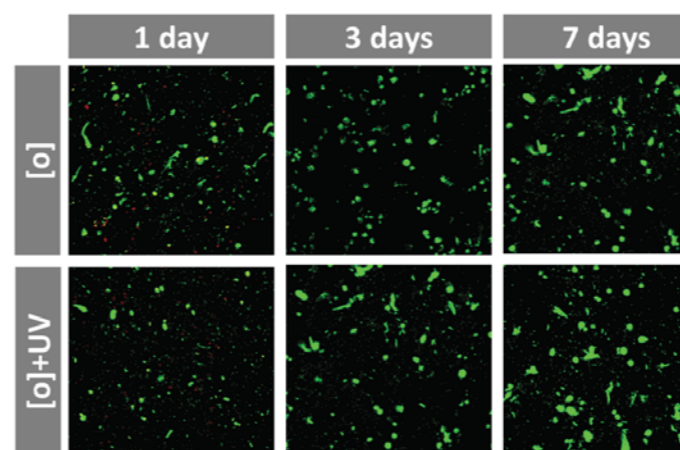


**Figure 8.** Live-Dead cell staining of SMCs encapsulated in blood vessel hydrogel after 1, 3 and 7 day culture. Two groups are oxidation crosslinking [O] and UV enhanced crosslinking ([O]+UV). Cells were stained with calcein-AM/ethidium homodimer, and living cells were detected as green fluorescence and dead cells were detected as red fluorescence.

## Cell Proliferation

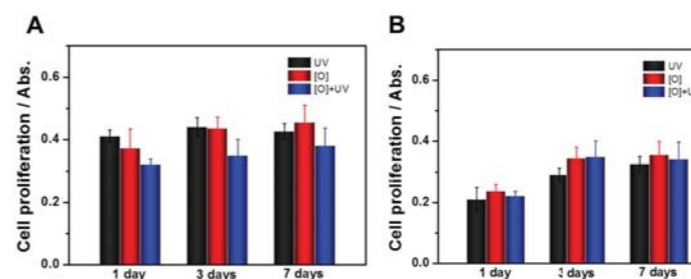


**Figure 9.** Cell proliferation was quantified by cell counting kit 8 (CCK-8). (A) SMCs were encapsulated in 3D bioprinted hydrogels. (B) HUVECs were seeded on the surface of the hydrogels. Three groups are UV crosslinking, oxidation crosslinking [O] and UV enhanced crosslinking ([O]+UV). Cell proliferation and absorbance was read at 450 nm via spectrometer. n=6, \*p<0.05. Data are expressed as mean ± standard deviation.

## Biological Analysis

### Dynamic Bioreactor Culture

In order to mimic surrounding fluid presented in vivo, a custom-designed flow bioreactor system was utilized to study the functions of 3D bioprinted blood vessels.

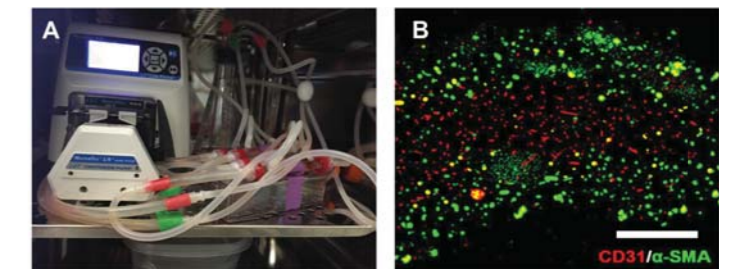


**Figure 10.** (A) Photo image of a custom-designed dynamic flow bioreactor system. (B) Immunofluorescence staining of 3D bioprinted blood vessel. The fluorescence image for alpha smooth muscle actin (α-SMA, green) and CD31 antibody (red) showed that the dual layer blood vessel construct exhibited excellent myogenesis and angiogenesis. The scale bars indicate 400 μm.

## Immunofluorescence Staining

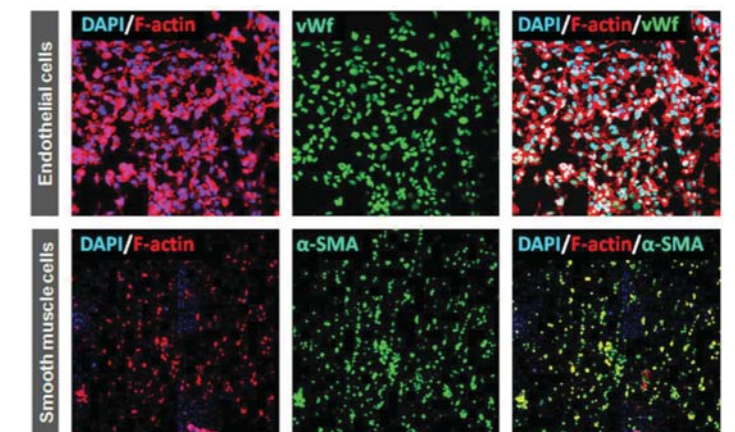


**Figure 11.** Locally amplified immunofluorescence staining of the 3D bioprinted blood vessels cultured in our bioreactor for 2 weeks. SMCs were encapsulated in 3D printed hydrogel, while HUVECs were grown on the surface of the hydrogels. The cells were stained with F-actin (red), nucleus (blue) and antibody (green) for von Willebrand factor (vWF) and α-SMA.

## Conclusion

In summary, the cell-laden bioinks can facilitate the printing of a self-supporting tubular structure and subsequent fabricating of the external tissue architectures without any patterned distortion. Moreover, the integration of 3D bioprinting technology with our tailored bioink effectively contributes to the creation of a novel, biomimetic, artificial blood vessel in 3D tissue implants for tissue and organ regeneration.

## Acknowledgements

This work is supported by NIH Director's New Innovator Award 1DP2EB020549-01.